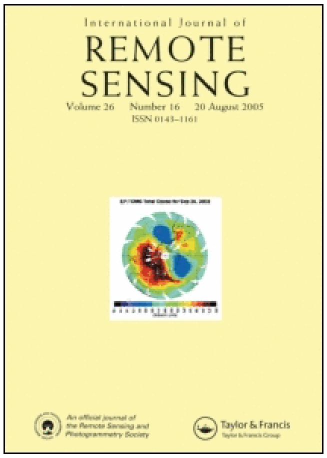

International Journal of Remote Sensing

Publication details, including instructions for authors and subscription information:
http://www.informaworld.com/smpp/title~content=t713722504

Distributions of surface water bodies

B.S. Daya Sagar [a]; M. Venu [a]; B. S. Prakasa Rao [a]
[a] Department of Geo-Engineering Andhra University, Visakhapatnam, India

Online Publication Date: 10 November 1995
To cite this Article: Sagar, B.S. Daya, Venu, M. and Rao, B. S. Prakasa (1995) 'Distributions of surface water bodies', International Journal of Remote Sensing, 16:16, 3059 - 3067
To link to this article: DOI: 10.1080/01431169508954608
URL: http://dx.doi.org/10.1080/01431169508954608

INT. J. REMOTE SENSING, 1995, VOL. 16, NO. 16, 3059–3067

Distributions of surface water bodies

B. S. DAYA SAGAR, M. VENU and B. S. PRAKASA RAO
Centre for Remote Sensing, Department of Geo-Engineering, Andhra University, Visakhapatnam – 530 003, India

(Received 9 November 1993; in final form 1 November 1994)

Abstract. A large number of digitized surface water bodies are automatically distributed on the basis of size and shape by performing an opening transformation. In addition, an iterated bisecting process is applied to construct self-similar size distribution of water bodies.

1. Introduction

The segregation of surface water bodies, on the basis of size and shape, is one of the important tasks of a hydrologist. Size distribution of any theme by means of manual methods, is tedious and time consuming. Moreover, by reducing the size of the water bodies, the technique of computing basic measures by means of planimetric analysis is laborious and inaccurate (Barker 1975). The size of each water body can be calculated to construct the size histograms. According to Delfiner (1972) size distributions of natural objects, like sand grains, are of three types: size distribution in measure, number and weight.

An opening transformation is one of the mathematical morphological concepts, in which erosion is followed by dilation (Serra 1982). This transformation, applied successfully to distribute different shapes depending upon the size of a population of sand grains (Delfiner 1972) and cervical cells (Meyer 1980), is adopted here to distribute automatically surface water bodies of different sizes. In size distribution studies the size of the structuring element plays a vital role. For instance, water bodies smaller than that of the considered structuring element will vanish leaving water bodies larger than the structuring element, after performing the opening operation. The opening transformation can be mathematically shown as:

$$[A \ominus \lambda B] \oplus \lambda B \neq \phi \qquad (\text{or}) A_{\lambda B} \neq \phi \tag{1}$$

$$[A \ominus (\lambda + \mu)B] \oplus (\lambda + \mu)B = \phi \tag{2}$$

This transformation is applied on a large number of surface water bodies to distribute them according to their sizes (symbols are given in the Appendix). In addition, a procedure based on iterated bisecting (Pietronero and Siebesma 1986, Schroeder 1990), is followed to construct the self-similar size distribution of surface water bodies. Both methods, the opening transformation and the iterated bisecting process, have been used independently in different disciplines (Delfiner 1972, Meyer 1980, Pietronero and Siebesma 1986, Schroeder 1990), but not in relation to the hydrological problem.

2. Sample study

The sample consists of a number of water bodies larger than (36·25 m by 36·5 m)n where (n should be more than 20 pixels). The limit 36·25 m × 36·25 m represents the smallest water body that could be traced accurately from IRS 1A (LISS II) data in geocoded format (see figure 1). It lies in between the geographical coordinates of 18°15′ an 18° 30′ N and 83° 30′ and 83° 45′ E, belonging to the 65 N/11 Survey of India topographic map. Since the resolution of IRS 1A (LISS II) data is 36·25 m by 36·25 m and the minimum limit considered is (36·25 m by 36·25 m)n, the water bodies not eliminated on the basis of this criteria are traced (figure 2). To carry out water body distribution studies automatically, all traced surface water bodies are digitized by a digital Pulnix camera. The water bodies, that are present in the major part of the image, are kept in the file of size 480 by 480 pixels (368·6 km by 368·6 km). By giving a specific threshold value, the entire data are kept in the form of water body and no-water body regions (figure 3).

3. Water bodies size distribution with respect to opening

Digitized data consist of surface water bodies of various sizes. To segregate them both in number, measure and weight, an opening transformation is performed by circular structuring elements of different diameters such as 5, 7, 9, 11, 13, 15, and 17 pixels. The structuring elements with 5, 7, and 9 pixels in diameter, are shown in figure 4. Other sizes follow similar patterns.

Figure 5 illustrates the opening of surface water bodies, with respect to these circular structuring elements. Different sizes and shapes of digitized water bodies are distributed according to their sizes by performing opening transformations by changing the radii of the circular structuring element. Successive stages in the opening transformation using circles of increasing diameter are shown as (*a*), (*b*), (*c*), and (*d*) in figure 5.

To compute size distribution (SD) functions of water bodies in number, measure, and weight, the following equations proposed by Delfiner (1972) are used.

$$\text{SD function in number, } F(d) = 1 - N[A_{\lambda B}]/N[A] \tag{3}$$

where $N[A]$ is the total number of water bodies in the original section.

$N[A_{\lambda B}]$ is total number of water bodies after opening with circular structuring elements of defined diameters.

$$\text{SD function in measure, } G(d) = 1 - V[A_{\lambda B}]/V[A] \tag{4}$$

where $V[A]$ is the total area of water bodies in the section. $V[A_{\lambda B}]$ is the surface area of the water bodies after opening with the circular structuring element of defined diameters.

$$\text{SD function in weight, } \phi(\Delta d) = \frac{(\pi(d/2)^2[N(A_{\lambda B}) - N(A_{(\lambda+(\mu-1))B})]}{V[A]} \times 100 \tag{5}$$

$$\text{(where } 0 \leq d \leq 17 \text{ pixels and } (\mu - 1) > 0)$$

The parameter weight (mass) is closely related to the volume in respect to water bodies. Volume can be computed from areas using the fractal dimension, on the basis of fractal-perimeter-length-area-volume relations (Mandelbrot 1982). Since the fractal dimensions of the perimeters of the water bodies in the present investigation are found to be similar (Sagar 1994), the depths of the water bodies are also assumed

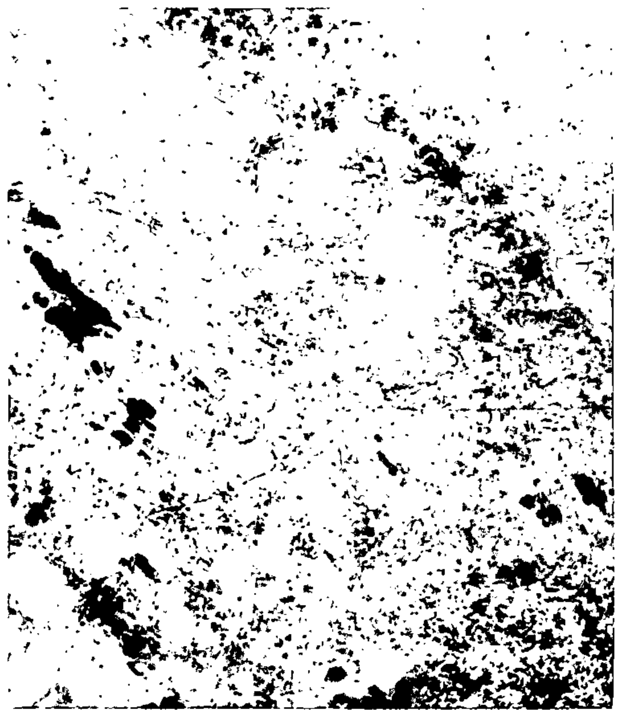

Figure 1. Geocoded IRS 1A (LISS II) data of 36·25 by 36·25 m resolution acquired on 3 August 1993.

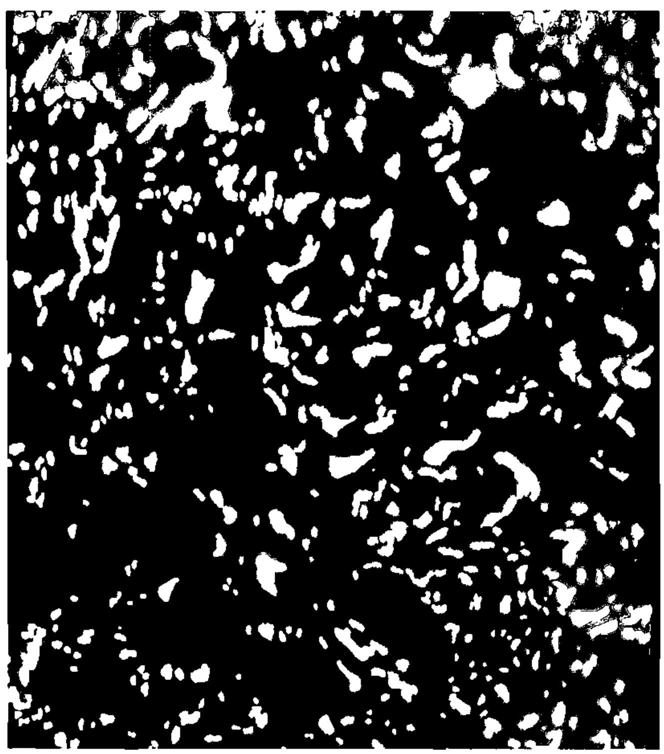

Figure 3. Data show surface water bodies in digital format.

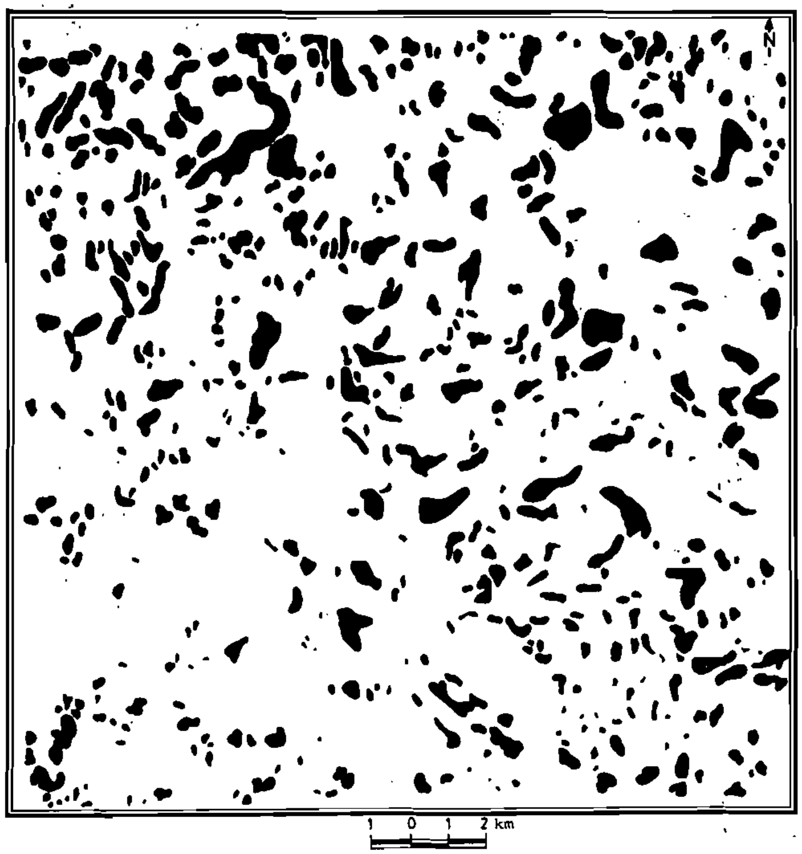

Figure 2. Traced water bodies from IRS 1A (LISS II) image.

```
    1 1 1
  1 1 1 1 1
  1 1 1 1 1
  1 1 1 1 1
    1 1 1
```
(a)

```
    1 1 1
  1 1 1 1 1
1 1 1 1 1 1 1
1 1 1 1 1 1 1
1 1 1 1 1 1 1
  1 1 1 1 1
    1 1 1
```
(b)

```
      1 1 1
    1 1 1 1 1
  1 1 1 1 1 1 1
1 1 1 1 1 1 1 1 1
1 1 1 1 1 1 1 1 1
1 1 1 1 1 1 1 1 1
  1 1 1 1 1 1 1
    1 1 1 1 1
      1 1 1
```
(c)

Figure 4. Circular structuring elements of different diameters. (*a*) 5 pixel diameter; (*b*) 7 pixel diameter; (*c*) 9 pixel diameter.

to be uniform, provided the area of the water bodies are the same. The appropriateness of such an assumption can be tested through the water bodies identified from digital elevation models, where one can compute the depth of the water body with more approximation. Volume can also be more accurately assessed through digital elevation models, where the depths can be computed with more approximation.

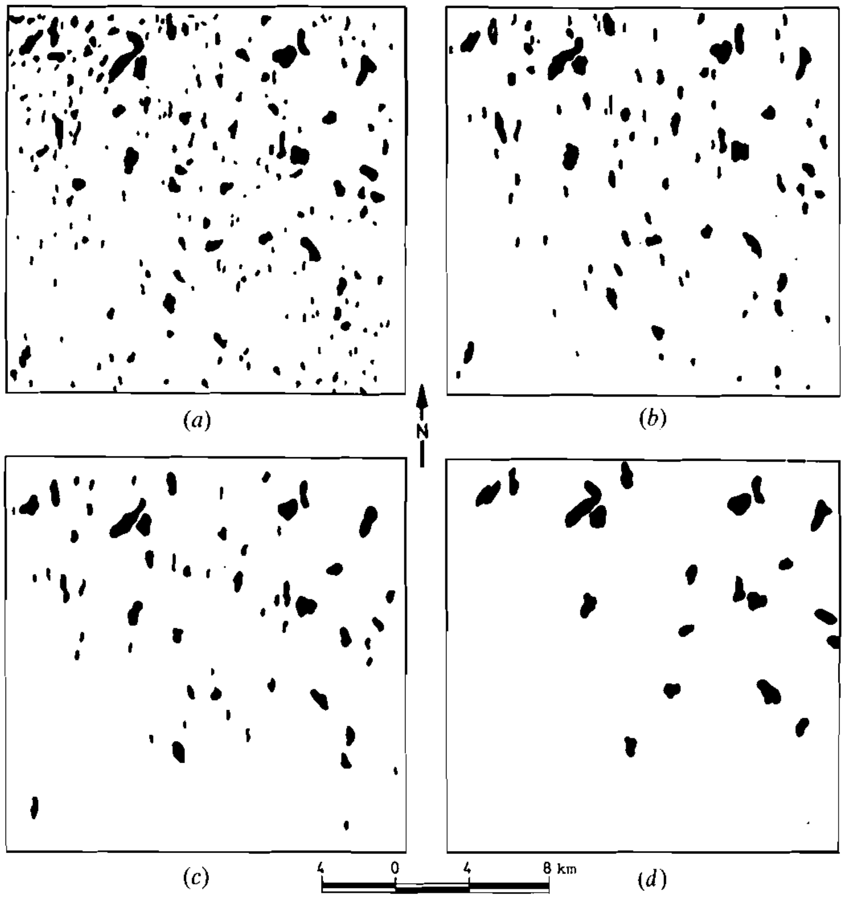

Figure 5. Evolution of water bodies under opening transformation by circular structuring elements with increasing radii.

In the above expression, d is the diameter of the structuring elements, ranging from 0 to 17 pixels. The expressions λ and $(\lambda+(\mu-1))$ represent different sizes, $\lambda<(\lambda+\mu-1))$, used for successive openings. The above expression may be used to arrive the size distribution in volume, since the density of water is same in respective categories of water bodies.

Table 1 records the size distribution functions of both number and measure. The weights of water bodies are expressed in histograms. The figures in the second column of table 1 record the size distribution functions of both number and measure. The weights of water bodies are expressed in histograms. The figures in the second column of table 1 indicate the proportion of water bodies with a diameter comprised of the corresponding line to that of the next. For example 19·08 per cent of the water bodies have a diameter between 7 and 9 pixels.

4. Self-similar distribution of water bodies by iterated bisecting

Iterated bisecting (Pietronero and Siebesma 1986) was adopted for the self-similar distribution of water bodies on the basis of latitude- and longitude-wise

Table 1. Size distribution functions of a section of surface water bodies.

Diameter of structuring element	SD function $F(d)\%$	Histogram $F(\Delta d)\%$	SD function $G(d)\%$	Histogram $G(\Delta d)\%$	WGTD $(\phi d)\%$
0	0	29·43	0	17·90	7·77
5	29·43	14·71	17·90	17·81	8·04
7	44·14	19·08	35·71	17·77	16·34
9	63·22	16·50	53·48	13·77	21·10
11	79·72	6·36	67·21	9·04	11·36
13	86·08	10·12	76·25	9·02	23·64
15	96·20	3·80	85·27	14·73	12·14
17	100·00	0·00	100·00	0·00	0·00

bisecting. Figure 7 shows three levels of bisecting on both latitude and longitude planes. This process begins with a uniform probability distribution over the unit interval (figure 8 (*a*) latitude bisecting; a_1: longitude bisecting). After bisecting the interval once, two probabilities, (1-P_1) and P_1, with the former less than the latter are obtained in single step distribution (figure 8 (*b*)(b_1)). Bisecting once more resulted in four intervals and the probability distribution is shown (figure 8 (*c*)(c_1)). A third bisecting results in the distribution shown (figure 8 (*d*(d_1)). In successively bisecting both longitudinally and latitudinally, the probabilities are represented as P_1, P_2, P_3...... Table 2 shows the values of $(1-P)$ and P at all levels of bisection both latitude and longitude-wise, (P;P_1, $(1-P_1)$; P_2, $(1-P_2)$; and P_3, $(1-P_3)$.

5. Analysis of results

The considered section of the basin consists of a large number of water bodies. The extent of similarities and differences between histograms of number, measure, and weight are shown in figure 6 (*a*)(*b*) and (*c*). Table 1 shows the values of size distribution functions in number, measure, and weights and those of the histograms. Considering the size distribution histograms for number ($F(\Delta d)\%$) and measure ($G(\Delta d)\%$) (figures 6(*a* and (*b*), for diameter of the structuring element $(d) < 11$ pixels $F(\Delta d)$ is found greater than $G(\Delta d)$ (except in between the diameters of 5 and 7

Table 2. Self-similar distribution of a section of water bodies.

Percentage area occupied by the total water body area											
Latitude-wise bisecting						Longitude-wise bisecting					
1st bisecting		2nd bisecting		3rd bisecting		1st bisecting		2nd bisecting		3rd bisecting	
0·51	0·49	0·24	0·26	0·11	0·14	0·63	0·37	0·35	0·28	0·19	0·15
(P_1)	$(1-P_1)$	$(1-P_2)$	(P_2)	$(1-P_3)$	(P_3)	(P_1)	$(1-P_1)$	(P_2)	$(1-P_2)$	(P_3)	$(1-P_3)$
		0·27	0·24	0·14	0·13			0·19	0·17	0·14	0·14
		(P_2)	$(1-P_2)$	(P_3)	$(1-P_3)$			$(1-P_2)$	(P_2)	$(1-P_3)$	(P_3)
				0·13	0·14					0·10	0·09
				$(1-P_3)$	(P_3)					(P_3)	$(1-P_3)$
				0·13	0·10					0·11	0·07
				(P_3)	$(1-P_3)$					$(1-P_3)$	(P_3)

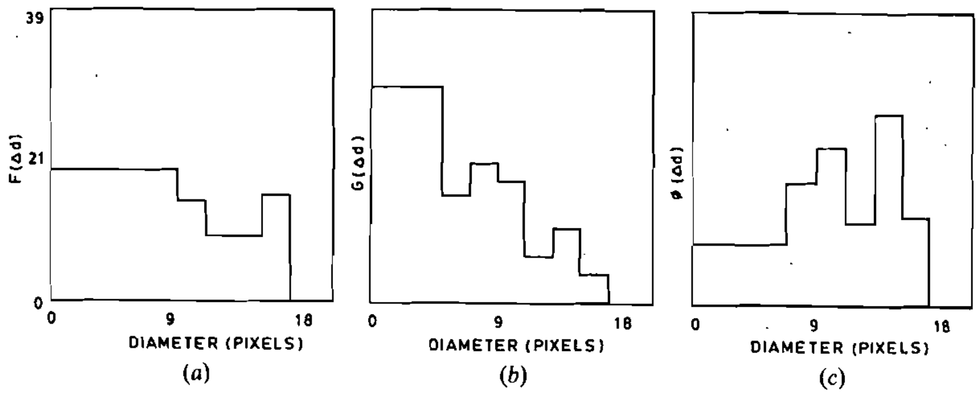

Figure 6. Histograms show (a) size distribution in number, $F(\Delta d)$, (b) size distribution in measure, $G(\Delta d)$, and (c) size distribution in weight, $\Phi(\Delta d)$.

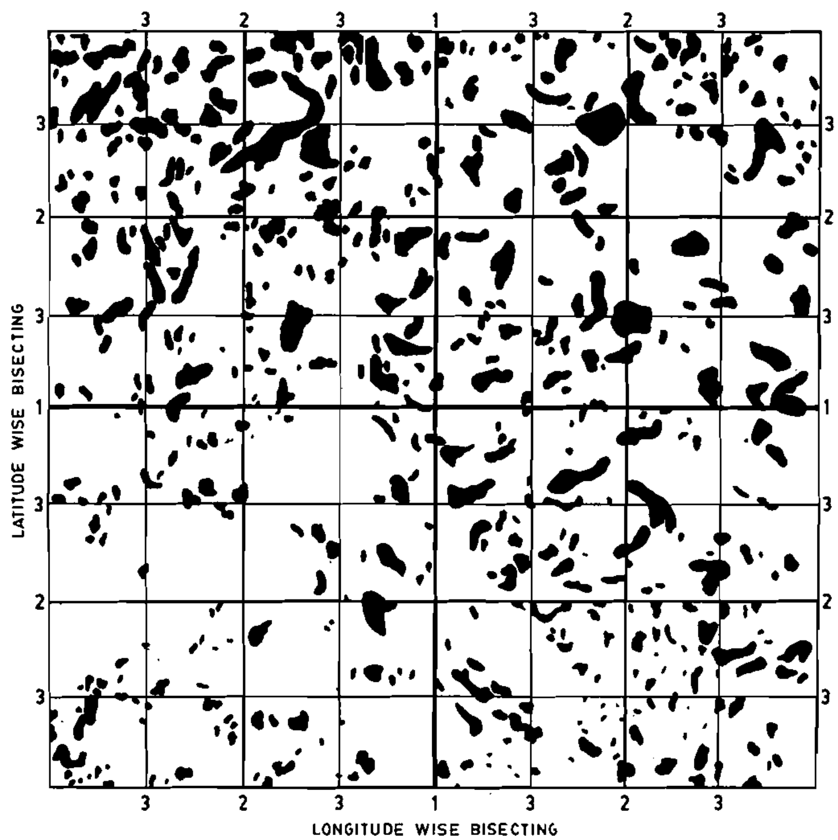

Figure 7. Section shows water bodies. Different bisecting lines both latitude and longitude wise. The digits 1, 2 and 3 on latitude and longitude planes represent successive levels of iterated bisecting to construct self-similar distribution of water bodies in figure 8.

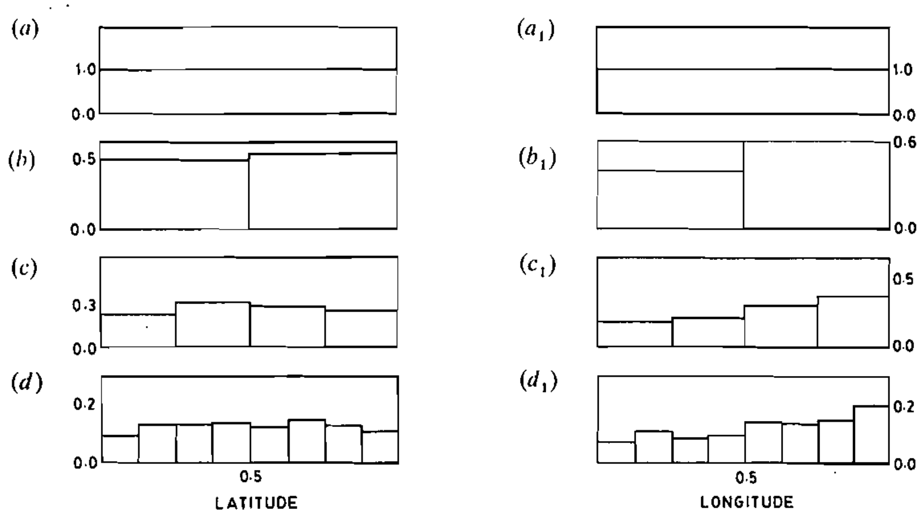

Figure 8. Self-similar distribution of water bodies by iterated bisecting, (*a*), (*b*), (*c*), (*d*) show latitude-wise bisecting and (a_1), (b_1), (c_1), (d_1) show longitude-wise bisecting.

pixels); thereafter $G(\Delta d)$ becomes greater because the few bigger water bodies contribute with a large area. Histograms ($G(\Delta d)$ with $\Phi(\Delta d)$ (figures 6(*a*) and (*c*)) exhibit similar behaviour except between 5 and 7, and at 9 and 11 pixels. Distribution of water bodies, through an iterated latitude-wise bisecting, is more or less uniform; whereas high variation is observed from P to $(1-P)$, at longitudinal bisecting. Three successive longitudinal bisectings in the study area result in eight regions, each with 28 000 pixels ($46{\cdot}08\,\mathrm{km}^2$) = 60 by 480 pixels ($2{\cdot}4\,\mathrm{km} \times 19{\cdot}2\,\mathrm{km}$); the uppermost region is the densest with 19 per cent of the total water body area. The lowermost region is the most sparse, with 7 per cent of the total water body area.

6. Conclusions

The size distribution of water bodies, which is very tedious by manual methods, is carried out with greater ease by opening transformation. This method for the size distribution of water bodies may be of use to hydrologists, limnologists and agriculturists in various ways. Besides this, self-similar distribution by iterated bisecting can be used to analyse the distribution of water bodies over a large area.

Acknowledgments

The authors gratefully acknowledge the suggestions given by Dr P. H. V. Vasudeva Rao. The facilities provided by the Indian Space Research Organisation (ISRO), India, under the RESPOND project, are also acknowledged. The senior research fellowship awarded by the Council of Scientific and Industrial Research (CSIR), India, is gratefully acknowledged by the first and second authors.

Appendix. List of symbols

$\ominus$	denotes erosion (shrinking)
$\oplus$	denotes dilation (expansion)
A	the object with set of points (water body pixels in this context) undergoing opening transformation

B	the structuring element is assumed to be bounded and closed.
$\lambda+\mu$	size of the structuring element greater than p, where μ is greater than zero.
$A_{\lambda B}$	indicates opening of A with respect to B of λ size; $A_B=(A\ominus\lambda B)\oplus\lambda B$.
ϕ	empty set.
$F(\Delta d)$	size distribution histogram (in number).
$G(\Delta d)$	size distribution histogram (in measure).
$\phi(\Delta d)$	size distribution histogram (in weights).
P & $(1-P)$	probability and unity minus probability.

References

BARKER, J. L., 1975, Monitoring water quality from Landsat. In *Proceedings of NASA Earth Resources Survey Symposium, Houston, Texas*, 1 A, pp. 383-418.

DELFINER, P., 1972, A generalization of the concept of size. *Journal of Microscopy*, **95**, 203-216.

MANDELBROT, B. B., 1982, *Fractal Geometry of Nature* (New York: Freeman).

MEYER, F., 1980, Feature extraction by mathematical morphology in the field of quantitative cytology. Technical report of Ecole nationale superiere des mines de Paris, Fountainbleau, France.

PIETRONERO, L., and SIEBESMA, A. P., 1986, Self similarity of fluctuations in random multiplicative processes. *Physical Review Letters*, **57**, 1098-1101.

SAGAR, B. S. D., 1994, Applications of remote sensing, mathematical morphology, and fractals to study certain surface water bodies. PhD thesis, Andhra University, India.

SCHROEDER, M., 1990, *Fractals, Chaos, Power Laws* (New York: Freeman).

SERRA, J., 1982, *Mathematical Morphology and Image Analysis* (London, New York: Academic Press).